EMI associated with inter-board connection for module-on-backplane and stacked-card configurations

X. Ye, J. Nadolny*, J. L. Drewniak, T.H. Hubing, T.P. Vandoren, D.E.DuBroff

Electromagnetic Compatibility Laboratory
Department of Electrical and Computer Engineering
University of Missouri – Rolla
Rolla, MO 65409
xiaoning@umr.edu
* AMP Incorporated, PO Box 3608, Harrisburg, PA 17105-3608, jim.nadolny@amp.com

Abstract: EMI associated with inter-board connection was studied through common-mode current measurements and FDTD modeling for stacked-card and module-on-backplane configurations. Three types of connections were investigated experimentally including an open pin field connection, an "ideal" semi-rigid coaxial cable connection, and a production connector. Both microstrip and stripline signal routing on the PCB were investigated. The results indicated signal routing on the PCBs or the inter-board connection can dominate the EMI process. Several cases of connector geometries were studied using FDTD modeling and good agreement was achieved between the measured and FDTD results.

I. INTRODUCTION

The module-on-backplane and stacked-card are both common configurations in high-speed digital designs. A typical module-on-backplane or stacked-card structure is of appreciable electrical extent, and functions as an EMI antenna at several hundred megahertz or higher. Three important aspects to be considered for understanding EMI related to inter-board connection include the connection itself, the signal routing on the PCBs, and the radiating EMI antenna. Previous work has been reported on the module-on-backplane connector [1], [2]. Numerical modeling of the EMI antenna has also been reported [3], [4]. However, work that includes all the three issues and their interactions is limited. The EMI coupling path, including the effects of the inter-board connection geometry and the PCB signal routing on the EMI, is demonstrated herein. FDTD is shown to be a powerful and useful modeling approach for analysis and design.

II. EXPERIMENTAL METHOD

Many studies found in the literature on the EMI performance of connectors focus on transfer impedance [2], [5], [6]. While transfer impedance is particularly useful for shielded connectors that mount in an enclosure wall, it is more ambiguous as a measure of EMI comparison for open region geometries such as interconnection of PCBs. Further managing measurement parasitics becomes challenging above approximately 500 MHz. In this paper, a simple common-mode current measurement technique was used [4]. This approach has the advantage that it is indicative of EMI, and allows direct and meaningful comparison of different connection geometries in the application environment. Further, the technique is an absolute method, so it provides a basis for comparison with modeled results.

The experimental setup is shown in Figure 1. A *0.085"* semi-rigid cable was attached to the test fixture and a Fischer-2000 clamp-on current probe was placed around the attached cable. The $|S_{21}|$ was measured with an HP 8753D network analyzer. The EMI was indicated by the measured common-mode current on the coaxial cable, which was related to $|S_{21}|$. The *60 cm × 60 cm* aluminum plate separated the test fixture from the measuring instruments to reduce the influence of the connecting cables and the human body, thereby enhancing the repeatability and dynamic range of the measurement. The probe response was compensated for in the network analyzer calibration procedure. The measured $|S_{21}|$ can be related directly to common-mode current as [4]

$$|S_{21}| = |150\Omega \cdot I_{CM}/V_{source}|$$

Other advantages of this experimental setup includes its low-cost; straightforward and easy implementation; repeatability; and can be used for evaluation of prototype and productive PCBs.

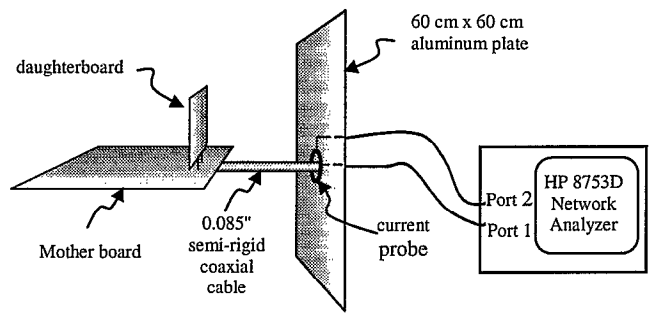

Figure 1. Schematic representation of the experimental setup for the common-mode current measurements.

This measurement method has been demonstrated for known configurations such as monopole antennas, and other simple radiating geometries that can be modeled numerically. The favorable comparison of the FDTD modeling and

measurements on inter-board connections presented herein also support the utility of this measurement approach.

III. EXPERIMENTAL STUDY OF INTER-BOARD CONNETIONS

A series of experiments was carried out on the module-on-backplane and stacked-card configurations using the measurement technique described in Section II. The objective was to discern the coupling mechanisms for the EMI associated with inter-board connections. For brevity, only the results for the module-on-backplane configuration will be presented in this section, since the coupling mechanism for these two configurations is similar. As indicated in Section I, critical issues for the inter-board connection study include the connection itself, the PCB trace routing, and the EMI antenna. In this series of experiments, three cases of inter-board connection were investigated: a simple open pin connection; an "ideal" semi-rigid coaxial cable connection; and a production connector. Microstrip and stripline signal routing on the PCBs were investigated. Previous reported results have shown that the PCB planes comprise portions of the EMI antenna and affect certain resonance frequencies [4].

A test fixture shown in Figure 2 (not uniformly scaled) was constructed for the experimental test-bed. A 0.085" semi-rigid coaxial cable was considered first as the "ideal" connection, which achieves near-perfect field containment at the inter-board connection. Both the motherboard and the daughterboard signals were routed in a stripline configuration formed by putting two *65-mil FR4* boards against each other. The size of the motherboard was *30 × 20 cm* and that of the daughterboard was *10 × 12 cm.* The signal was fed by an attached *20-cm 0.085"* semi-rigid cable into a *2-cm 50 Ω* trace on the mother-board, and directed through the connection into a *5-cm 50 Ω* trace on the daughterboard, then terminated by a *47 Ω* SMT resistor. The common-mode current on the attached cable was measured using the setup shown in Figure 1. The result is shown in Figure 3, together with the result for all the edges of the stripline configuration shielded with copper-tape. The sharp spikes in the measurements result in part from the environmental noise, since the experiment was not conducted in a shielded room. Since the semi-rigid cable had good field containment at the connection, the effective EMI source mechanism was dominated by the signal routing on the PCB, even though it was a stripline geometry. With all the edges shielded, the measured common-mode current was reduced nearly to the noise floor.

The $|S_{21}|$ results for the stripline PCB routing configuration with an open pin connection are shown in Figure 4. The measured common-mode current with all the edges of both boards shielded with copper tape was not significantly different from the result without the shielding. In this case, the connection was the dominant EMI coupling mechanism. Results in Figures 3 and 4 are two ends of a spectrum, but indicate that either the signal routing on the PCBs or the inter-board connection can dominate the EMI coupling path. In practical applications where EMI is attributed to signal routing between PCBs, first discerning which feature is dominating the EMI coupling path is critical to successful mitigation of a problem.

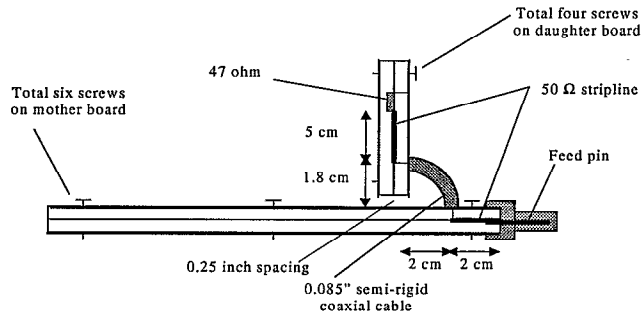

Figure 2. Test fixture geometry for a stripline PCB routing configuration with an ideal semi-rigid cable connection

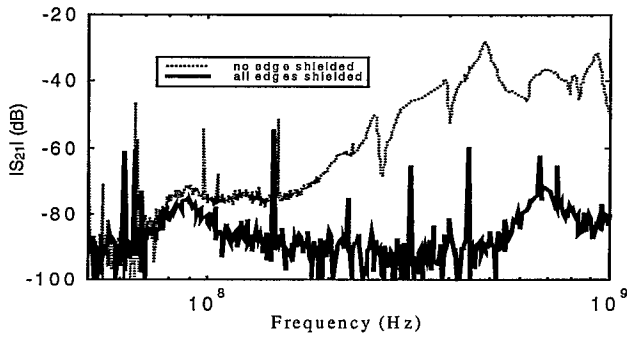

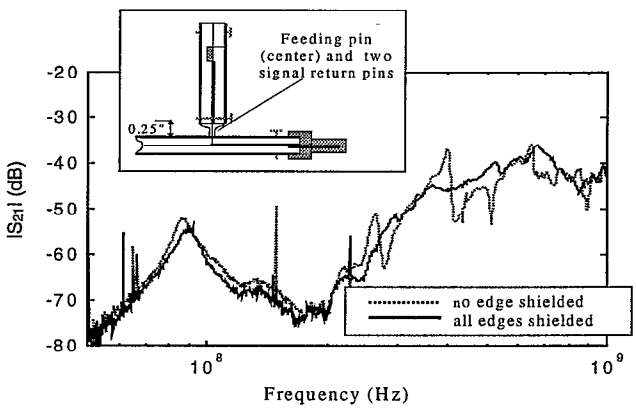

Figure 4. Measured results for a stripline PCB routing configuration with an open-pin connection

A high-performance production connector was then tested. The HS3 (AMP, Inc.) connector was a stripline-type, multi-pin connector with each row of pins sandwiched between two conductor blades [7]. Each ground blade had 3 short contacts which were used for the connection between the ground blade and PCB ground plane or power plane. The EMI performance

of this connector was studied from several perspectives. First, a comparison of the EMI performance between the configurations with an ideal connection and an HS3 connector was conducted. The geometry of the mother board and daughterboard was the same as that in Figure 2, except that a *31-mil* substrate was used for both types of connection, and the shorting screws were replaced by shorting copper-tape for convenience. Only one slice of the HS3 connector assembly was used for ease of soldering. For both types of connection, the relative position of the PCBs remained the same, so that the results are directly comparable. The measured $|S_{21}|$ for stripline PCB routing is shown in Figure 5a. Another comparison was made for microstrip signal routing on the PCBs and the result is shown in Figure 5b. In both cases, the lines were *50 Ω*, and checked with TDR measurements. The signal was routed through the connector on an outer pin row (see Pin-out A in Figure 7) with the longest routing path through the connector, which was the worst case for EMI concerns.

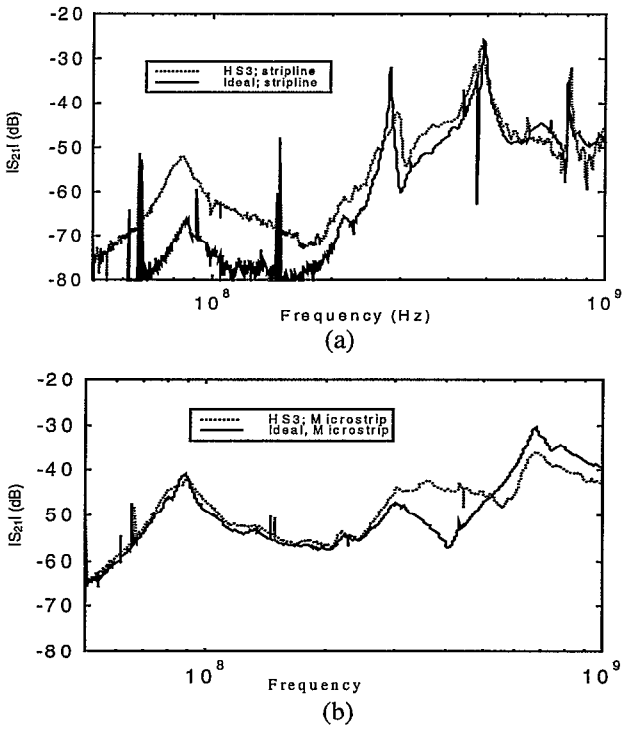

Figure 5. Comparison of the "ideal" connection and HS3 connector for: (a) stripline PCB routing, and (b) microstrip PCB routing.

The results in Figure 5a indicate that a stripline-type connector configuration is close to ideal and the EMI mechanism is dominated by PCB level effects. Below 100 MHz the HS3 connection does not achieve the performance of the ideal connection because the coupling mechanism is dominated by magnetic field effects, or the finite inductance of the connection. The field containment is near perfect for the semi-rigid coaxial cable, and while superior for the HS3, does not achieve this. Though high-performance stripline type connectors such as the HS3 are intended for use above several hundred megahertz and not below 100 MHz, this difference emphasizes that magnetic field effects are dominant in the lower frequency range. However, as the frequency increases beyond 200 MHz, both magnetic field and electric field coupling are significant, and the performance of the stripline type connector achieves that of the "ideal" case. The common-mode current peaks at approximately *300, 500, and 800 MHz* result from radiation (from the planes) at the resonances of the parallel planes of the stripline configuration. These resonances could be shifted by shorting pins (analogous to decoupling capacitors with the correct resonance frequency). Though these resonances are particularly high Q here, it is expected that in a populated board the Q will be considerably smaller. The introduced resonance frequencies were increased as the number of the shorting pins increased. These results agree well with studies on the effects of shorting posts on microstrip antennas [8].

For microstrip routing on the PCB, the performance of the two connections is comparable in the frequency range below 200 MHz as shown in Figure 5b, indicating that the radiation is dominated by PCB level EMI mechanisms [9], [10], [11]. The peaks at approximately *90, 300, and 650 MHz* result from EMI antenna resonances associated with the PCB planes and the attached cable [12]. Above 200 MHz, the performance of the ideal and stripline-type connections are comparable, with approximately 5 dB differences in the resonant peaks. The significance of electric-field, as well as magnetic-field coupling at the higher frequencies is further supported by the crossing of the measured results at high frequencies for the ideal and HS3 connections. Namely, the measured common-mode current for the ideal connection exceeds that for the HS3.

The stripline-type routing path through the connector provides superior field containment at the connection area, and aids in minimizing EMI. A comparison between a stripline-type connector routing path and a microstrip-type connector routing path was also made to investigate the advantage of this approach. The microstrip-type connector routing path was achieved by removing one of the ground conductor blades adjacent to the signal pin. Both stripline and microstrip signal routing on the PCB were considered for the two different connection configurations. The shortest connector signal routing path was used, which was also on an outer pin row. The measured common-mode current for stripline and microstrip routing through the connector is compared in Figure 6. The measured common-mode current for the stripline PCB signal routing case was approximately 10 dB greater for the single ground return blade (microstrip routing through the connector) than for the dual ground return blades sandwiching the signal (stripline routing through the connector). This significant difference is a result of the decreased field containment, and increased impedance with the single-blade return. Further, since the PCB level EMI mechanisms are minimized with stripline signal routing,

reducing the field containment, i.e., increasing the impedance of the return has a large effect on the measured common-mode current. By contrast, however, EMI mechanisms on the PCB are dominant for microstrip signal routing on the PCB for the bladed return type connector. Consequently, there is relatively little difference in the measured common-mode current for the stripline and microstrip routing path through the connector. The non-uniform difference in the measurements, as well as the crossing in the results at high frequencies again emphasizes the fact that both electric- and magnetic-field coupling is important.

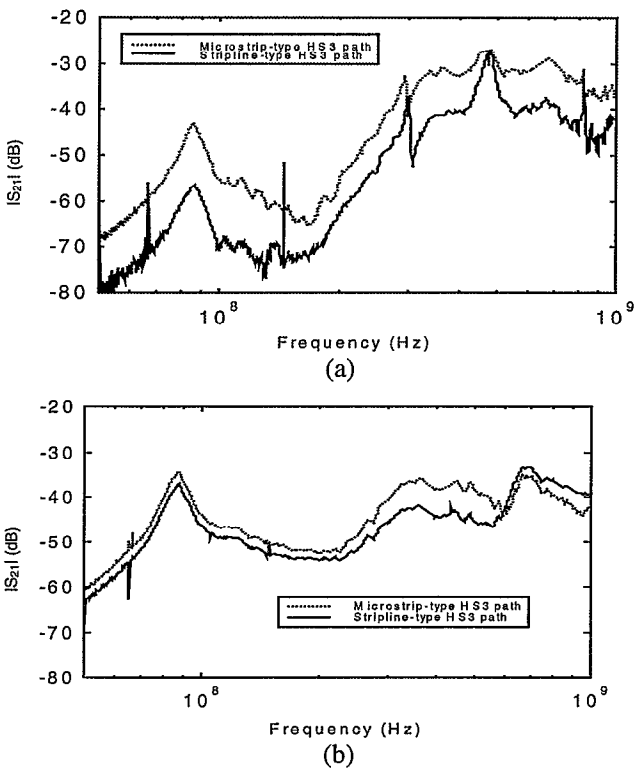

Figure 6. Comparison of the measured common-mode current for the stripline-type connector routing path and microstrip-type connector routing path: (a) stripline PCB trace routing, (b) microstrip PCB trace routing.

There are totally six signal pins in each row of the HS3 connector. The effect on EMI of different pin positioning was also studied. In order to focus on the performance of the connection itself, a configuration without traces on the PCB was used. The signal was fed from the motherboard, directed through the connector, and shorted to the daughterboard. Two cases of pin positioning were selected for study, one with the connector signal routing path at the edge of the connector, and the other at the center. The pin-out of the connector and the comparison of the measured $|S_{21}|$ are shown in Figure 7. The results are expected since case B has better field containment than case A. Further, the uniform difference in the measured common-mode current up to 600 MHz indicates that the effect is dominated by magnetic-field containment up to this frequency (since magnetic field effects dominate at low-frequencies).

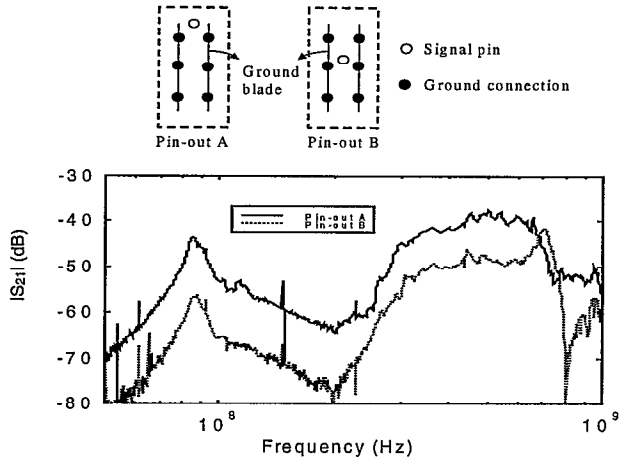

Figure 7. Measured common-mode current for different signal pin positions.

Experiments on the stacked-card configurations were also conducted, and the relevant physics was similar to the module-on-backplane configuration. Some of the results are presented in the next section.

IV. FDTD MODELING

Numerical modeling of the EMI associated with inter-board connections was also done. The objectives are to have a better understanding of the physics of the problem, demonstrate the measurement technique, and provide direction for connector and PCB designs. As the experimental studies detailed in the previous section have indicated, a full wave analysis incorporating both magnetic and electric-field coupling is necessary. FDTD was utilized as the modeling tool. The FDTD method was chosen because of the capability for analyzing multiple frequencies with a single time-domain simulation, and further, it is well suited for rectilinear geometries.

Due to the complexity and mixed scales (both large and small dimensions) of the problem, modeling the entire problem including traces on PCBs and the fine details of the connector geometry requires an excessive number of unknowns and computation time. At this stage, the modeling of the PCB traces on PCB was not yet included. Stacked-card configurations with different inter-board connections and a typical module-on-backplane configuration were built for comparison of the modeling to measured results. There was no trace on the PCBs and the study focused on EMI the performance of the connection.

The test fixture of the stacked-card configuration is shown in Figure 8. The dimensions of the motherboard and daughterboard were the same as those shown in Figure 1, and

the length of the attached semi-rigid cable was *20 cm*. The spacing of the two boards was *2 cm* and the offset between them at the connection edge was *0.5 cm*. The outer shield of the semi-rigid cable was soldered to the ground plane of the motherboard. Three types of inter-board connection, shown in Figure 8, denoted A, B and C, were studied. For case A, two AWG 24 wires were used as the connection, one as signal pin and the other as the ground return. The signal pin was *2 cm* away from the right edge of the motherboard. The spacing between the signal pin and the return pin was *2 mm*. Connection B was a symmetric geometry with three ground return pins on each side of the signal pin. The spacing between any two adjacent pins was *2 mm*. Connection C came from Connection B by attaching a *1.2 cm × 1.2 cm* copper tape patch to each row of the ground return pins, mimicking the ground blade approach of the stripline-type connector.

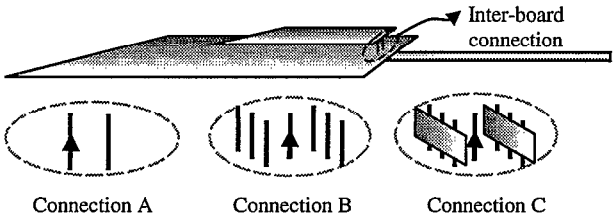

Figure 8. The stacked-card configuration and geometry of inter-board connections

The plied, using a uniform cell size of *2 mm ×2 mm ×2 mm*. The PCB planes were modeled as perfect electric conductors and a thin wire algorithm was used to model the wire strucures in the fixture [13]. Eight perfectly matched layers (PML) were placed at each boundary plane of the computational domain [14], and the number of white space layers between the PML and test fixture was seven. The *60 cm ×60 cm* aluminum plate was modeled as an infinite ground plane. The dielectrics on the PCBs were omitted. Figures 9a, b and c show the modeled and measured common-mode current results for the stacked-card configuration with Connections A, B, and C, respectively. Good agreement was achieved between the modeled and measured results. The discrepancies at low-frequencies are due in part to pre-mature termination of the FDTD simulation and an FDTD time history that was not sufficiently long. Consistent with the previous experimental results, these results indicate that the ground blade approach provides superior EMI performance.

A module-on-backplane was also modeled and constructed for measurements. The configuration geometry is shown in Figure 10. Two pieces of AWG24 wire with a right-angle bend were used as the inter-board connection, one as signal pin and the other as the ground return. The common-mode current on the attached cable is compared for the measured and modeled results in Figure 11. The agreement is again good.

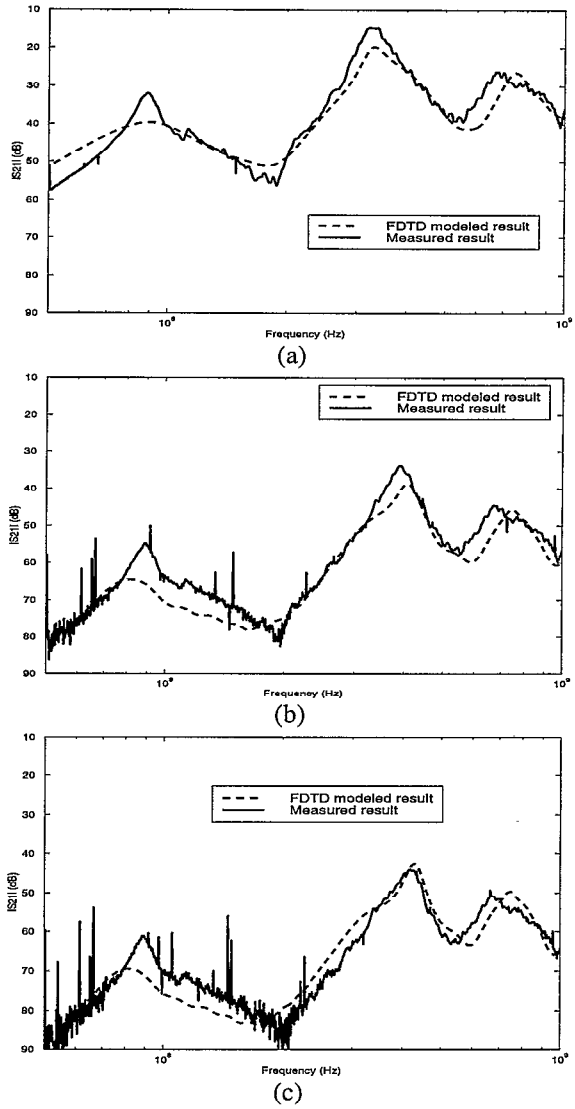

Figure 9. Modeled and measured common-mode current results for the stacked-card configurations: (a) Connection A; (b) Connection B; and, (c) Connection C.

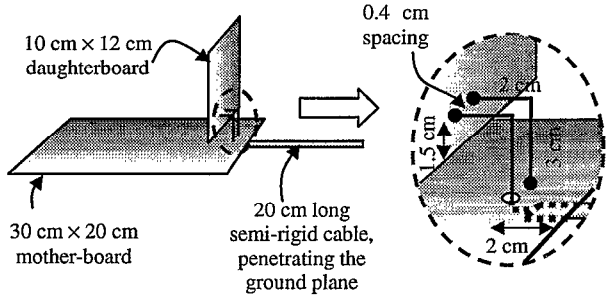

Figure 10. Geometry of the module-on-backplane configuration.

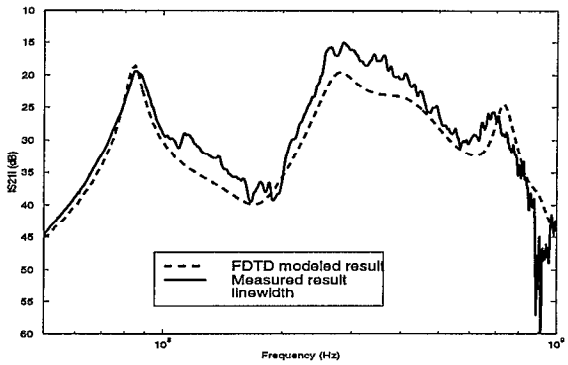

Figure 11. Modeled and measured common-mode current for the module-on-backplane configuration of Figure 10.

V. SUMMARY AND CONCLUSIONS

A test and measurement method was developed to study EMI associated with inter-board connection. The relevant physics was investigated by a series of experimental studies. The FDTD method was demonstrated to be a suitable modeling tool, with good agreement between the modeled and measured results. There are several conclusions that can be drawn from the present studies. First, the common-mode current approach is a suitable experimental method for evaluating prototype and production connectors and connector pin designations for EMI performance, as well as prototype or production PCBs for determining the dominance of PCB or connection effects in any EMI problem. Second, PCB level EMI mechanisms or the inter-board connection can dominate EMI associated with a motherboard/daughterboard configuration. The EMI performance of the stripline type connection studied herein was superior, and for microstrip signal routing on the PCB, the common-mode current on the attached cable was dominated by PCB level EMI mechanisms. Both E- and H-field coupling contributed to the EMI performance of the connection. Consequently, simple maxims for "improving" the EMI performance of a connector geometry may be inadequate for addressing the complex coupling at high frequencies. The FDTD method is a powerful modeling approach, and was shown to be suitable for modeling inter-board connections. This approach provides a means for better understanding of the relevant coupling physics at high frequencies, and developing connector designs with quantified EMI performance. Further, the modeling can provide insight when meaningful experiments are difficult to construct.

REFERENCES

[1] Larry K.C. Wong, "Backplane connector radiated emission and shielding effectiveness," *IEEE Int. Symp. Electromagn. Compat.*, pp346-351, 1994.

[2] B. Vanlandschoot, L.Martens, L. Van den Torren, D. Morlion, "An improved triaxial cell for transfer impedance measurements on multipins backplane connectors," *IEEE Int. Symp. Electromagn. Compat.*, pp141-144, 1997.

[3] Kevin Li, M. Ali Tassoudji, Soon Y. Poh, Michael Tsuk, Robert T. Shin, Jin Au Kong, "FDTD analysis of Electromagnetic Radiation from Modules-on-backplane configuration," *IEEE Trans. Electromagn. Comp.*, vol. 37 no. 3, pp326-332, Aug. 1995.

[4] David M. Hockanson, James L. Drewniak, T.H. Hubing, T.P. Van Doren, Fei Sha, Michael J. Wilhelm, "Investigation of fundamental EMI source mechanisms driving common-mode radiation from printed circuit boards with attached cables," *IEEE Trans. Electromagn. Comp.*, vol. 38, no. 4, pp557-565, Nov. 1996.

[5] L. O. Hoeft, J. S. Hofstra, "Measured electromagnetic shielding performance of commonly used cables and connectors," *IEEE Trans. Electromagn. Comp.*, vol. 30 no. 3 pp 260-275, Aug. 1988.

[6] S. Dunwoody, E. VanderHeyden, "Transfer impedance testing of multi-conductor shielded connectors of arbitrary cross-section" *IEEE Int. Symp. Electromagn. Comp.* pp 581-585, 1990.

[7] http://www.amp.com.

[8] W.F.Richards, "Microstrip Antennas", Chapter 8 in *Antenna Handbook: Theory, Applications, and Design*, Edited by Y.T.Lo and S.W.Lee, Van Nostrand Reinhold, New York, 1988.

[9] D. M. Hockanson, C. W. Lam, J L. Drewniak, T H. Hubing, T P. Van Doren, "Experimental and numerical investigations of fundamental radiation mechanisms in PCB designs with attached cables," *IEEE Int. Symp. Electromagn. Comp.*, pp305-310, 1996.

[10] Christopher L. Holloway, Edward F. Kuester, "Net and partial inductance of a microstrip ground plane," *IEEE Trans. Electromagn. Comp.* vol. 40, no. 1, pp 33-46, Feb 1998.

[11] F. B. M. van Horck, A. P. J. van Deursen, "Prediction of common-mode currents on cables connected to a multilayer printed circuit board and couplings," on *the board EUT Report*, Eindhoven University of Technology, Faculty of Electrical Engineering. n 97-E-305, pp 1-53, Aug 1997.

[12] David M. Hockanson, James L. Drewniak, Todd H. Hubing, Thomas P. Van Doren, and Richard E. DuBroff, "FDTD and experimental investigation of EMI from stacked-card PCB configurations," accepted by *IEEE Trans. Electromagn. Comp.*

[13] A. Taflove, "The Thin Wire", Chapter 10 in *Computational Electrodynamics: The finite-difference time-domain method,* Artech House Publishers, Boston-London.

[14] J. P. Berenger, "Perfectly matched layer for the absorption of electromagnetic waves," *J. Comput. Phys.*, vol. 114, pp.185-200, Oct. 1994.